FEA-Assisted Analysis and Gain Optimization of a Micromechanical Resonant Displacement Amplifier

Gleb Melnikov
Clark Nguyen, Ed.

Electrical Engineering and Computer Sciences
University of California at Berkeley

Technical Report No. UCB/EECS-2017-207
http://www2.eecs.berkeley.edu/Pubs/TechRpts/2017/EECS-2017-207.html

December 13, 2017

FEA-Assisted Analysis and Gain Optimization of a Micromechanical Resonant Displacement Amplifier

by Gleb Melnikov

Research Project

Submitted to the Department of Electrical Engineering and Computer Sciences, University of California at Berkeley, in partial satisfaction of the requirements for the degree of **Master of Science, Plan II**.

Approval for the Report and Comprehensive Examination:

Committee:

Clark T.C. Nguyen

Professor Clark T.-C. Nguyen
Research Advisor

12/13/17

(Date)

* * * * * * *

Professor Kristofer S. J. Pister
Second Reader

12/13/17

(Date)

Table of Contents

List of Figures

List of Tables

Acknowledgements

First and foremost, I would like express my sincere gratitude to Professor Clark Nguyen for his tremendous support and guidance throughout my graduate research career. Without his mentorship, I would not have been able to complete this project.

I am grateful to my colleagues Alper Ozgurluk, Kieran Peleaux, Kyle Tanghe, Alain Anton, Thanh-Phong Nguyen, Qianyi Xie and Yafei Li for the encouragement and assistance they have given me throughout this project and the courses we have taken together at UC Berkeley.

I am also indebted to all of the faculty at UC Berkeley who have provided me with a world class education. In particular, I would like to thank Kris Pister for his outstanding introductory course to the fascinating world of MEMS.

Lastly, I would like to thank Shirley Salanio for the phenomenal work she performs on a daily basis as a graduate advisor.

Abstract

Micromechanical resonant switches have the potential to greatly outperform currently dominant semiconductor switches due to their higher figures of merit. Of the current designs available, resonant MEMS switches are among the most promising, as they can achieve very large amplitudes at resonance with greatly reduced actuation voltages compared to more conventional MEMS switches, such as those that rely on pull-in based actuation.

Such resonant micromechanical devices are currently in their infancy, and require additional optimization and analysis to resolve their unique issues and become useful in commercial applications. In this study, finite element analysis and SPICE circuit simulation have identified the potential for optimal displacement amplification through the variation of coupling beam length for a recently proposed displacement amplifier topology. Through the simulation of several disk-based displacement amplifier designs, an optimal configuration was found that may achieve use in power converters and switch based amplifiers of the future.

Chapter 1

Introduction

Owing to their extremely high quality factors, low input capacitance, and ability to act as conductive switches, capacitively transduced micromechanical resonators have the potential to drastically change the landscape in RF communication and power circuits. MEMS based switches have demonstrated a considerably higher figure of merit (FOM) than their transistor-based counterparts due to an additional degree of freedom not available to semiconductor switch designers (the gap), and the ability to use air as a dielectric. They have also demonstrated better isolation and lower insertion loss [1].

1.1 Background

The resonant micromechanical switch, or resoswitch, is of particular interest for use in switching converter and power amplifier applications, as it has demonstrated far greater switching speeds than competing MEMS switch technologies [2]. By utilizing nonlinear dynamical properties and large displacement amplitudes at resonance, the resoswitch solves many of the issues associated with previous micromechanical switches, including low switching speed and high actuation voltage, and has the potential for increased reliability [3]. Current resoswitch technologies are not without their own set of problems, however.

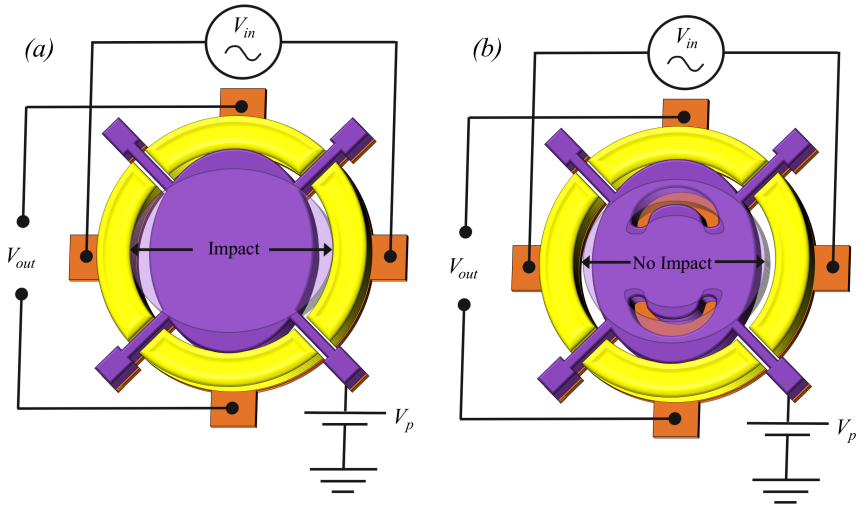

Figure 1: (a) Wineglass resoswitch without displacement amplification, where both input and output electrodes impact, and (b) with displacement amplification, with only input electrodes impacting.

Previous designs all have a fair amount of compromises. For example, in an early design demonstrated in Figure 1 [3], during resonance, the input electrodes also impact in addition to the output electrodes. This would

create complications in many potential applications for such a switch, as the input signal would be tied directly to the output periodically.

The second design in Figure 1 demonstrates a later modification that was able to address the input electrode impacting issue with the design in Figure 1 through the use of stiffness engineering [4]. By etching slots into part of the resonator, the stiffness is selectively reduced more in one direction than the other, thus achieving displacement amplification in primarily one direction of motion.

Unfortunately, this design comes with its own severe drawbacks. In particular, the quality factor of the device is reduced due to the distorted asymmetrical wineglass modeshape, and the center frequency is shifted considerably because overall the stiffness is reduced more than the mass. Both of these are troublesome. High quality factor is one of the most desirable attributes of these resonators, and it is problematic that the modified center frequency currently lacks an analytical expression.

1.2 Motivation and Objective

A more recent design, proposed in [5], has demonstrated the capability to solve both of these problems by utilizing digitally specified stiffness engineering. This design is displayed along with sample circuits for potential applications in Figure 2. By utilizing an input array of radial contour mode resonators that move in unison and act as one effective resonator with increased stiffness by a factor of 4, coupled to a single output disk, this design achieves a theoretical displacement gain of 2. This allows the output disk to impact but not the input disk, without significantly degrading the

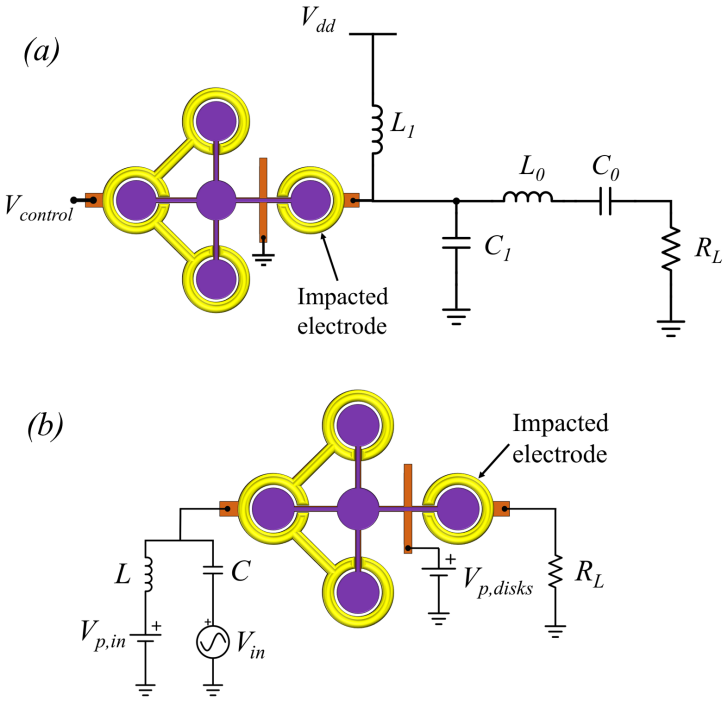

Figure 2: (a) Class E amplifier circuit utilizing resonant displacement amplifier and (b) switching power amplifier circuit.

modeshape and thus preserving the high quality factor of the disk resonators [5].

This switch design also offers another potential advantage over the wineglass disk in resoswitch applications, in that due to the uniform radial motion of the radial contour modeshape, the impact surface area (and thus the effective conductive surface area) is considerably larger. Contact resistance can frequently result in multiplication in resistance by as much as four orders of magnitude for micromechanical switches [1]. This is an important consideration, as high contact resistance has historically been an issue for micromechanical switches.

Several notable challenges potentially exist with this design. The displacement gain is much smaller than that of the wineglass disk (which achieved a displacement magnification of 7.94x through the use of gain stages in [4]), leaving less margin of safety to prevent possible input electrode strikes. This issue is further complicated by the fact that the input disks frequently do not truly move in perfect unison and some have larger displacement amplitudes than others. In pursuit of obtaining a more optimized and functional MEMS resoswitch, this work studies the characteristics of this micromechanical resonant displacement amplifier design with the intent of optimizing performance for such applications as shown in Figure 2 by maximizing displacement gain and amplitude.

1.3 Overview

First, equivalent circuit that describe the structure are provided in Chapter 2 for use in SPICE simulations, the results and details of which are provided in Chapter 3. Chapter 4 describes FEA analysis studies performed and the results obtained. Finally, the conclusions of this study are provided in Chapter 5.

Chapter 2

Equivalent Circuits

With the intent of creating a simplified model that can be simulated relatively quickly and easily using SPICE software, an equivalent circuit that converts mechanical domain signals into their electrical equivalents is frequently utilized to aid in the design of resonant micromechanical devices. In the case of electromechanical circuits such as the MEMS resonator-based devices described in this report, relevant circuit performance, such as gain, frequency response, and impedance, can be directly obtained from the SPICE simulations.

2.1 Radial Contour Mode Disk Resonator

We begin with the basic model for a capacitively-transduced disk resonator. The equivalent circuit for such a device, obtained from the electromechanical analogy between the differential equations for a second order mass spring system, is a series LRC resonant tank with transformers to couple the electrical and mechanical domains [6]. This circuit is shown in Figure 3 below. The equations used to solve for the equivalent circuit parameters are provided in Table 1 immediately following the figure [7-9].

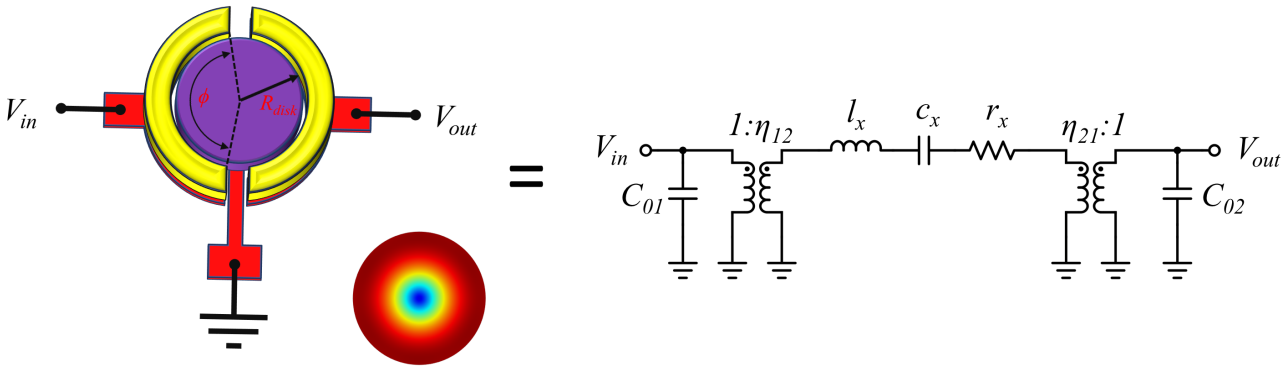

Figure 3: Radial contour mode disk resonator equivalent circuit.

Table 1: Equivalent Circuit Parameters

$r_x = c_{re} = \frac{\omega_0 m_{re}}{Q}$ (1)	$C_0 = \frac{\varepsilon t \phi R_{disk}}{g_0}$ (5)
$c_x = \frac{1}{k_{re}} = {\omega_0}^2 m_{re}$ (2)	$m_{re} = \frac{2\pi\rho t}{J_1^2(hR_{disk})} \int_0^{R_{disk}} r J_1^2(hr)\, dr$ (6)
$l_x = m_{re}$ (3)	$h = \sqrt{\frac{{\omega_0}^2 \rho}{\frac{E}{1+\sigma} + \frac{E\sigma}{1-\sigma^2}}}$ (7)
$\eta = V_p \frac{\varepsilon t \phi R_{disk}}{{g_0}^2}$ (4)	

In the above equations, R_{disk} represents the disk radius, g_0 the gap size, σ the Poisson's ratio, ρ the density, ε the permittivity, t the thickness of the resonator, ϕ the resonator angle swept by the electrode, V_p the applied dc bias, ω_0 the natural frequency, Q the quality factor, and E the Young's modulus. J_1 is the Bessel function of the first kind, of order 1.

2.2 Extensional Mode Coupling Beam

The extensional (axial) mode coupling beams used to couple radial contour mode disk resonators together can be modeled by a general two port transmission line T-model, as shown in Figure 4 [10].

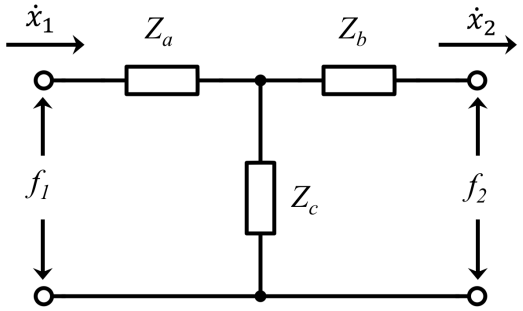

Figure 4: Transmission line T-model of extensional mode coupler.

Assuming that the motion is purely extensional, this T-model can be described by the *ABCD* impedance matrix given below [6].

$$\begin{bmatrix} f_1 \\ \dot{x}_1 \end{bmatrix} = \begin{bmatrix} \cos \alpha L_c & \dfrac{j \sin \alpha L_c}{Z_0} \\ jZ_0 \sin \alpha L_c & \cos \alpha L_c \end{bmatrix} \begin{bmatrix} f_1 \\ \dot{x}_1 \end{bmatrix} = \begin{bmatrix} A & B \\ C & D \end{bmatrix} \begin{bmatrix} f_1 \\ \dot{x}_1 \end{bmatrix} \tag{8}$$

where

$$Z_0 = \frac{1}{A\sqrt{\rho E}} \tag{9}$$

$$\alpha = \frac{\omega}{v_e} \tag{10}$$

$$v_e = \sqrt{\frac{E}{\rho}} \tag{11}$$

L_c is the length of the coupling beam, A is the cross sectional area, ρ is the density, ω is the frequency, and E is the Young's modulus. To obtain the impedances of interest in the equivalent circuit, this matrix can be solved by equating to a chain network, as in [11, 12], and solving for series and shunt impedances.

$$Z_a = Z_b = \frac{A-1}{C} = \frac{\cos \alpha L_c - 1}{jZ_0 \sin \alpha L_c} = \frac{k_{sa}}{j\omega} \tag{12}$$

$$Z_c = \frac{1}{C} = \frac{1}{jZ_0 \sin \alpha L_c} = \frac{k_{sc}}{j\omega} \tag{13}$$

These impedances may be represented as capacitors, since capacitance is the inverse of stiffness in the mechanical to electrical analogy.

$$c_{sa} = c_{sb} = \frac{1}{k_{sa}} = \frac{1}{\omega} \frac{Z_0 \sin \alpha L_c}{\cos \alpha L_c - 1} \tag{14}$$

$$c_{sc} = \frac{1}{k_{sc}} = \frac{Z_0 \sin \alpha L_c}{\omega} \tag{15}$$

2.3 Displacement Amplifier

By coupling radial contour mode disk resonators using the extensional mode couplers described above, a multiple order filter can be created. The displacement amplifier that is the

subject of this work is one such filter. Its simplified equivalent circuit is provided below. This device consists of 4 input radial contour mode disks coupled by λ/2 length beams, at which the effective coupling impedances reduce to zero and thus allow the four disks to form a single effective "composite resonator", in which both the stiffnesses and the masses of the input disks are added. Thus, these couplers are effectively replaced by wires. An output disk is coupled to the input disks by a coupler of a length that will be varied in this study. Note that η_{12} in Figure 5 is three times as large as η_{12}, as there are 3 input electrodes and only one output. Also note that l_{x1}, c_{x1}, and r_{x1} represent the composite resonator formed by summing the 4 individual resonators in series.

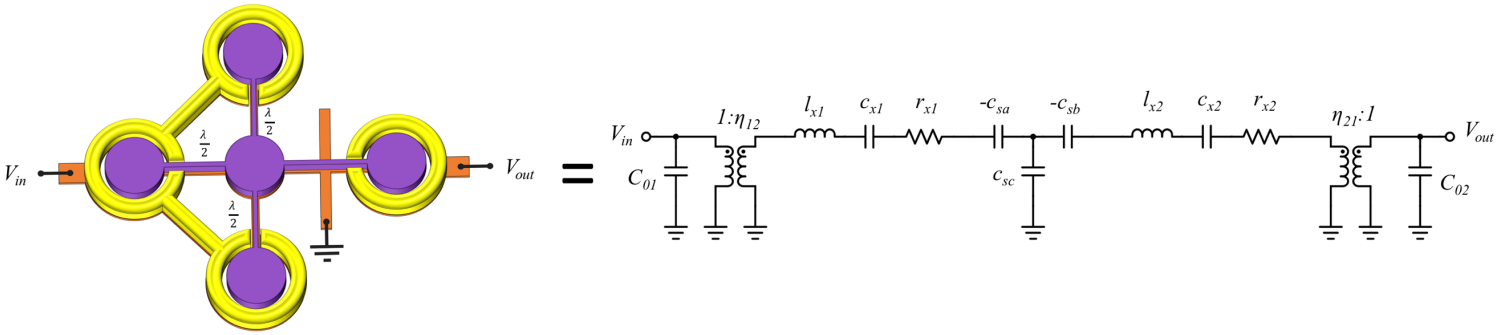

Figure 5: Displacement amplifier equivalent circuit.

This device achieves displacement gain due to the difference in effective stiffness between the effective single composite resonator input disks and the output disk. The peak displacement gain for this amplifier is provided simply by the square root of the ratio of the number of input disks to the number of output disks [5]:

$$\frac{X_o}{X_i} = \sqrt{\frac{N_i}{N_o}} \tag{16}$$

Chapter 3

SPICE Analysis

Equivalent circuits parameters were obtained through the use of a Python script that calculates the values, using equations (1) to (7), along with (14) and (15). This script would then automatically output a netlist file and call SPICE from the command line to run it. This highly automated process allows for multiple calls to SPICE to be made in one script, and requires only that the user enter the desired resonator specifications. Such an approach enables rapid simulation of various circuit configurations and automatic generation of numerous plots.

The dimensions of the structures simulated, along with all of the calculated equivalent circuit parameters and other relevant values pertaining to the displacement amplifier, are provided in Table 2. These same values are used for the remainder of the simulations in this report.

Table 2: Displacement Amplifier Parameter Summary

Parameter	**Value**	**Units**
Disk Radius, R_{disk}	17.23	μm
Center Frequency, f_0	153.2	MHz
Structural Layer Thickness, t	3	μm
Gap, g_0	100	nm
Coupler Width, W_c	1	μm
Wavelength, λ	52.71	μm
DC Bias, V_p	7	V
AC Stimulus, V_i	0.1	V
Elastic Modulus, E	150	GPa
Density of Polysilicon, ρ	2300	kg/m^3
Poisson's Ratio, σ	0.226	-
Resonator Quality Factor Q	10500	-
r_x	$4.507 \cdot 10^{-7}$	Ω
c_x	$2.195 \cdot 10^{-7}$	F
l_x	$4.916 \cdot 10^{-12}$	H
$\eta_{12} = \eta_{21}$	$2.014 \cdot 10^{-6}$	C/m
Electrode Capacitance, C_0	$5.754 \cdot 10^{-14}$	F

Figure 6 plots the effect of changes in coupler length on the frequency response of this circuit. This circuit acts as a filter, with two distinct peaks visible for all coupler lengths that are not integer multiples of λ/2. For coupler lengths between λ/2 and 3/4λ, the peaks are both shifted right and the higher peak eventually moves far to the right and disappears as the coupler length approaches λ/2. Conversely, for coupler lengths longer than 3/4λ, the upper peak eventually becomes the single resonant peak at lambda.

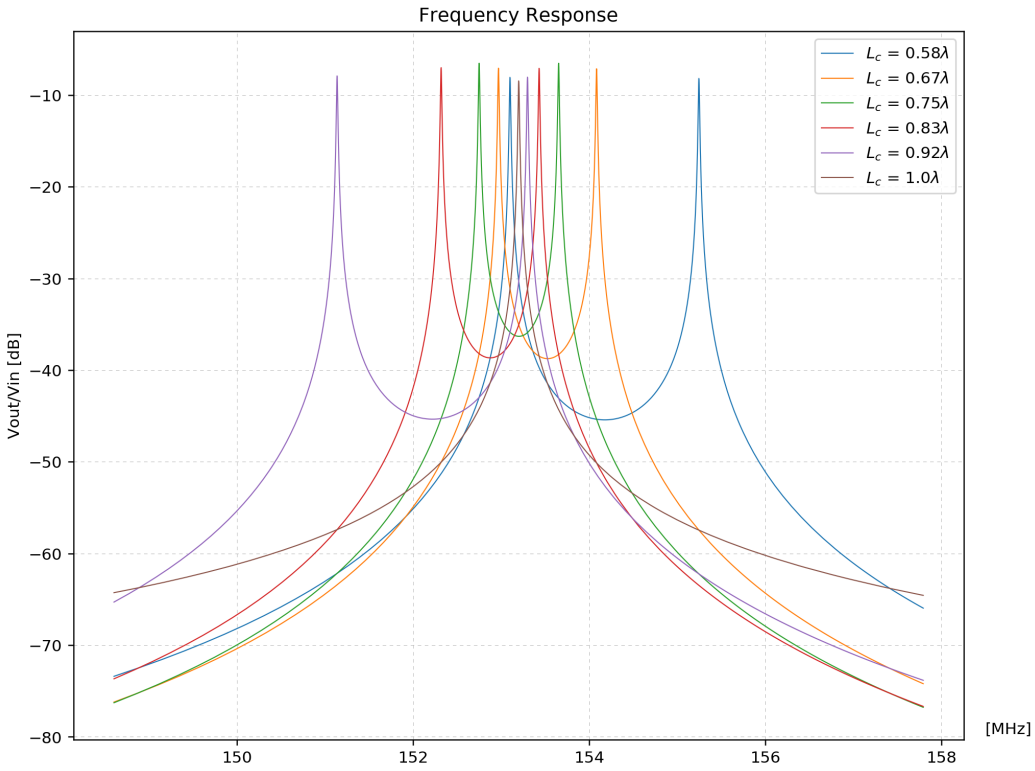

Figure 6: Effect of coupler length on frequency response.

Figure 7 shows the input and output impedances pertaining to the displacement amplifier for a range of coupling lengths from λ/32 to 1.5λ. As this filter produces two distinct peaks in its frequency response, impedances are measured at both the low frequency and high frequency mode peaks.

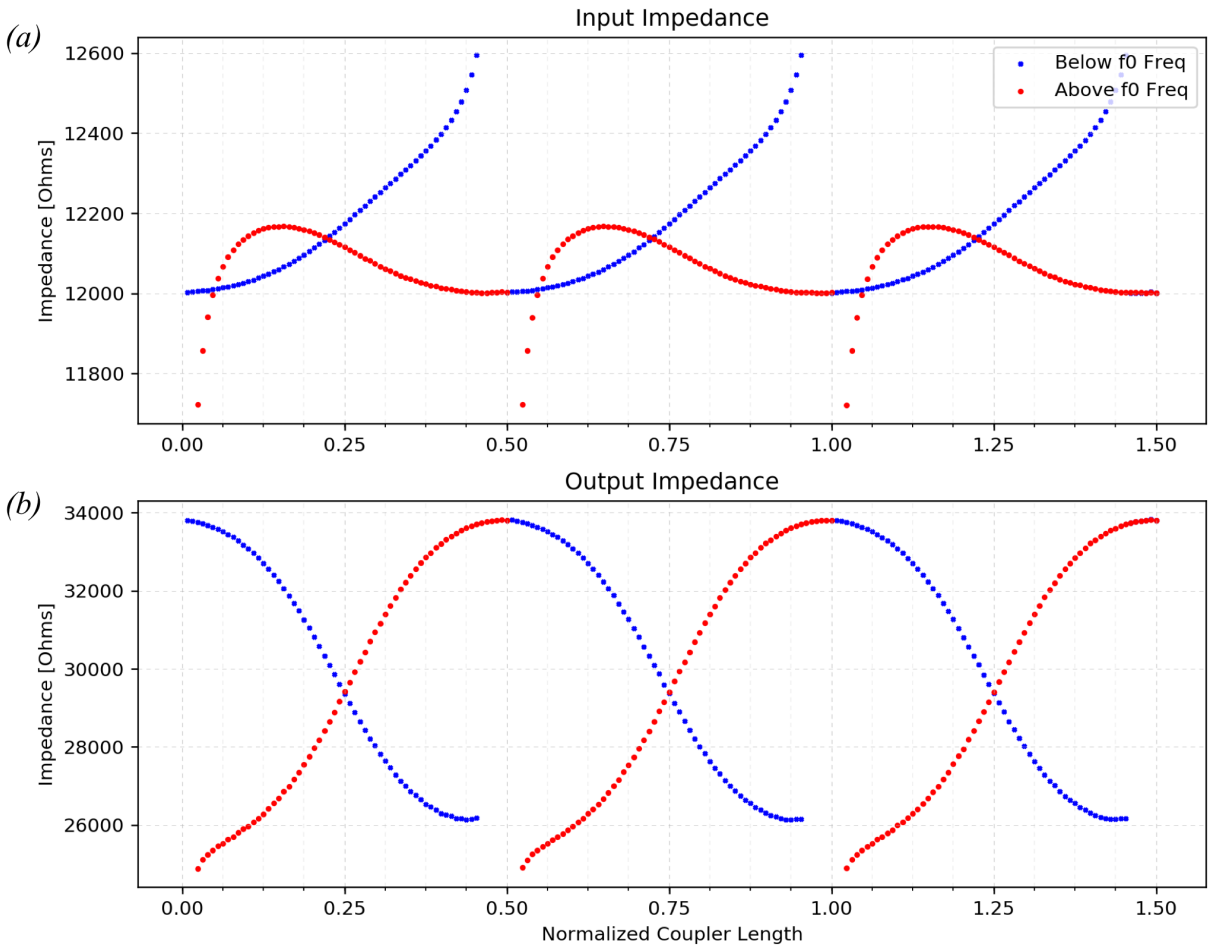

Figure 7: (a) Input and (b) output impedances.

Chapter 4

FEA Analysis

With the pursuit of optimizing the performance of this displacement amplifier for use in resoswitch applications, as well as gaining a better understanding of the characteristics of this device and verifying its characteristics, FEA simulations were performed using COMSOL software. Prestressed eigenfrequency simulations, followed by prestressed frequency domain studies, were conducted in order to obtain the desired dataset.

4.1 Prestressed Eigenfrequency Analysis

In order to identify the normal modes of this device and measure the relative displacement gains from input to output, an eigenfrequency study was first performed. As expected, there are two primary mode shapes, one in which the input and output disks expand and contract in phase, and one out of phase, as shown in Figure 8. Note that numerous other spurious modes also exist for this device in the vicinity of the center frequency, however, such modes will not be excited by the electrode configuration used for this design, which does not apply appreciable out of plane forces. Thus, these data points have been ignored in this study.

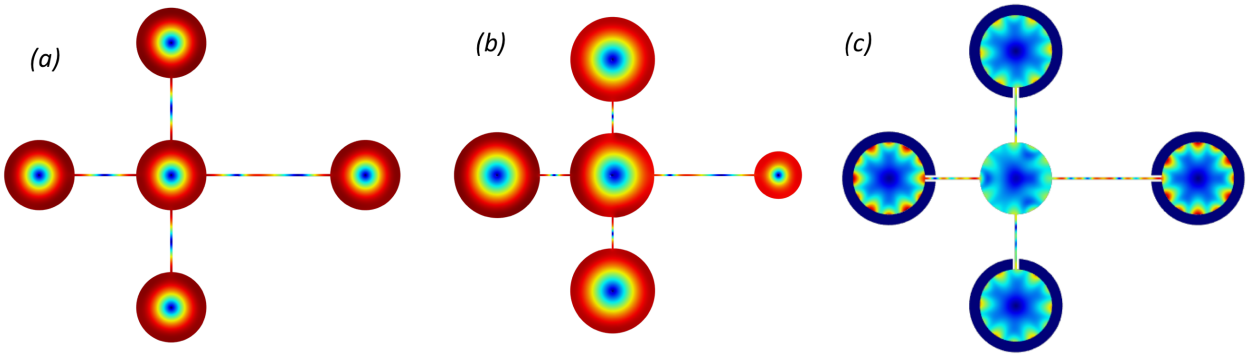

Figure 8: (a) In phase modeshape, (b) out of phase modeshape, and (c) spurious mode, shown with enclosing electrodes.

The setup for this study is shown in Figure 9. Symmetry boundary conditions were applied with the intent of removing some unwanted spurious mode shapes and improving simulation times. The resonators are held in place with perfectly aligned stems that have fixed boundary conditions

on their lower boundaries. The entire structure is enclosed in a nonsolid vacuum domain with a deformable mesh to allow for electric field lines to permeate. To speed up simulation time while allowing for accurate measurement of desired values, a custom mesh was used with an extremely fine mesh in the small gap to ensure accurate measurement of small displacements. As the gap is 100 nm, the minimum element size for the gap region was set to 90 nm, in order to ensure the mesh is smaller than the minimum feature size.

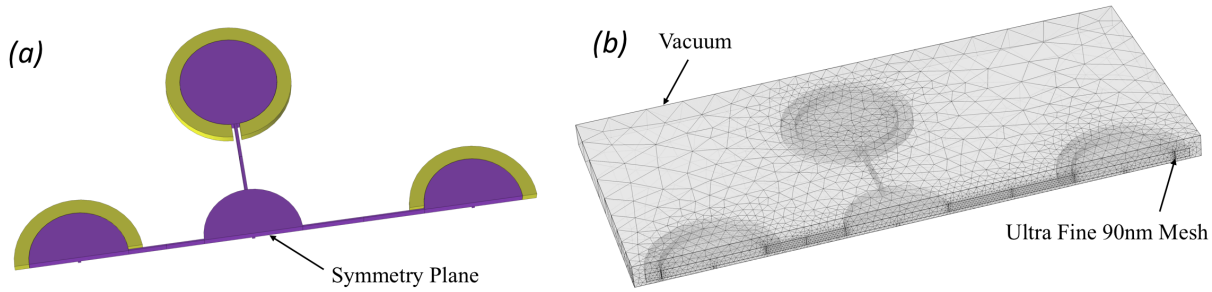

Figure 9: (a) Top view of the structure in the simulation setup, showing input and output electrodes and symmetry plane, and (b) a meshed isometric view demonstrating extremely fine meshing in the small gap and vacuum enclosure.

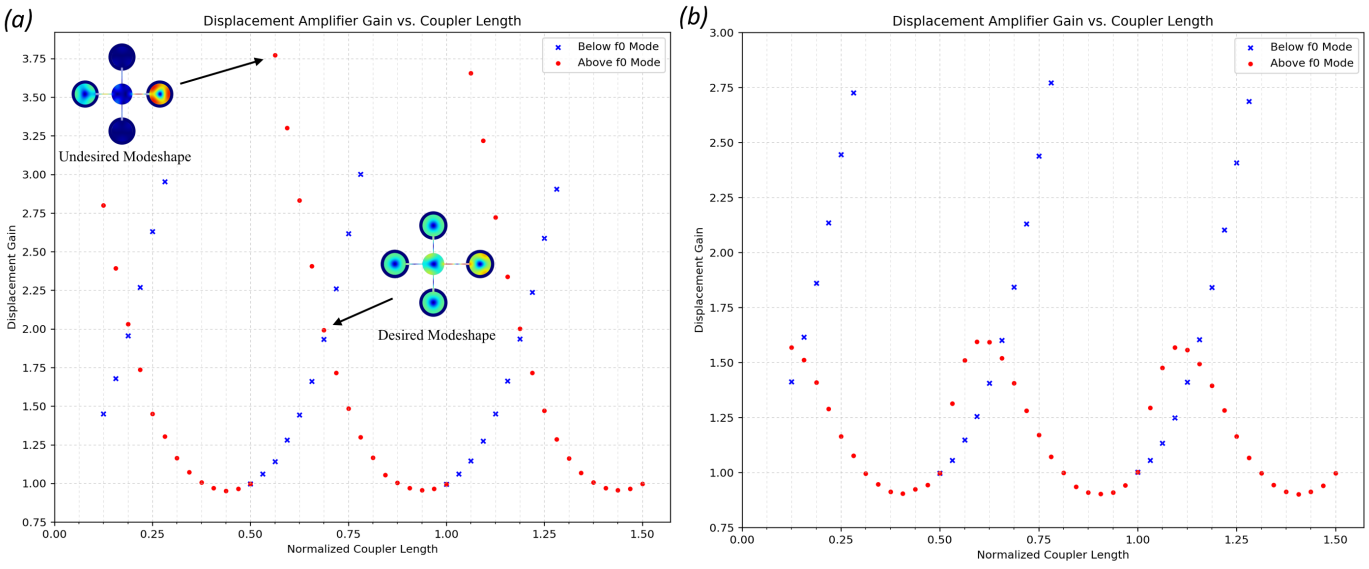

Figure 10: Displacement amplifier gains measured relative to (a) average input disk displacement and (b) largest input disk displacement.

Displacement gain was found by dividing the maximum radial displacement of the output disk by the maximum displacement of the input disks. This was done for both peaks. For many cases, the input disks did not all share the same displacement magnitude. In particular, for coupling lengths close to multiples of λ/2, the high frequency mode primarily only excites the disk opposite of the output disk. This is quite undesirable, as this would result in input disk impacts. To obtain meaningful gain results from this data, two plots were created, one that takes the average of the maximum displacement of the four input disks, and one that uses the maximum individual disk value. Figure 10 depicts these two plots.

From these plots, it is evident that the low frequency mode exists only between integer multiples of approximately λ/2 and λ/4. For comparison, an amplifier with only one input disk and one output disk was also simulated, and was found to produce an expected gain of unity across all lengths. The relevant plot may be found in the appendix.

4.2 Prestressed Frequency Domain Analysis

The results obtained from the eigenfrequency study, while insightful, are inconclusive as an absolute maximum displacement amplitude cannot be obtained from such a study. The displacement gains plotted from this study are somewhat questionable for this given application as some of the undesirable modeshapes may not be actuated by the given electrode configuration. The frequencies of normal modes obtained from the eigenfrequency study were saved and used to perform frequency domain sweeps within the vicinity of said frequencies, with the intent of measuring absolute output displacements.

For the remaining frequency domain studies performed, inputs are applied as voltages on the electrodes.

In order to obtain meaningful displacement peak amplitudes, it is necessary to apply damping to the mechanical structure. Losses in such structures are well modeled by Rayleigh material damping in COMSOL, and are a function of the quality factor and frequency of the device. Thus, the remainder of the simulations in this study were performed with Rayleigh damping applied assuming a quality factor of 10500.

As simulation accuracy is of foremost importance when measuring absolute displacements, an analysis was first performed on a single disk resonator and compared to expected values from

theory. For a fully enclosed disk resonator, the maximum radial displacement at resonance is given by:

$$R_{peak} = \frac{QF_i}{k_{re}} \tag{17}$$

where

$$F_i = V_p V_i \frac{\partial C}{\partial r} = V_p V_i \frac{C_0}{g_0} \tag{18}$$

and k_{re} and C_0 are given in Table 1.

For the radial contour mode disk resonator used throughout this work, excited by a $0.1V_{ac}$ input, the predicted maximum displacement from (17) is 464.45 pm. The FEA frequency domain study yielded a maximum displacement of 466.10 pm. Only a 0.36% difference, this is an excellent match between theory and simulation, and demonstrates that the mesh is sufficiently fine enough for the simulation to be accurate. Details regarding the setup of this simulation can be seen in Figure 11. For this simulation, two symmetry boundary conditions were used along xz and yz planes.

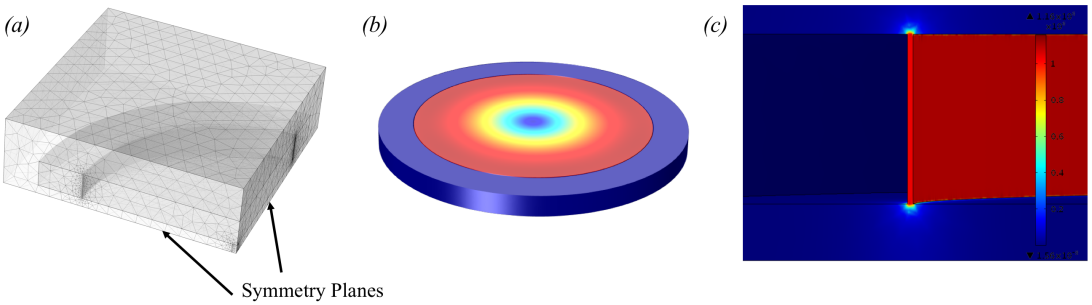

Figure 11: (a) Fully enclosed single resonator meshed structure with two planes of symmetry, (b) resonator mode shape, and (c) close up view of gap e-field demonstrating sufficient mesh resolution for high accuracy. As expected, the e-field measures ~1 MV/m.

In order to avoid the challenge of calculating gain that is defined relative to input disks with different displacement amplitudes, as was the case in the eigenfrequency study, additional sweeps were performed for a single pair of resonators coupled as shown in Figure 12. This would provide a reference with which to compare the displacements.

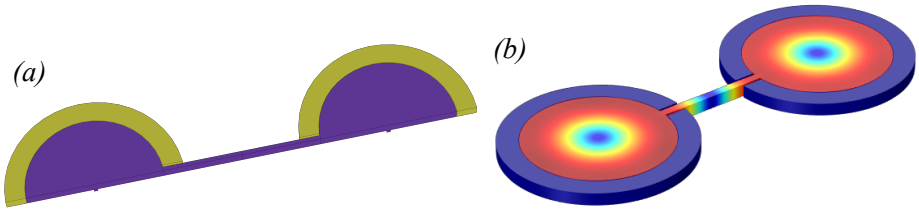

Figure 12: (a) Single input and output disk FEA analysis setup, and (b) mode shape.

As in the eigenfrequency study, displacement values were measured for both low and high frequency peaks. As the displacements and gains are periodic for integer multiples of λ/2, as demonstrated by the previous eigenfrequency study displacement plots, simulations were only conducted for lengths between λ/2 and λ. Figures 13 and 14 show the results obtained from these studies.

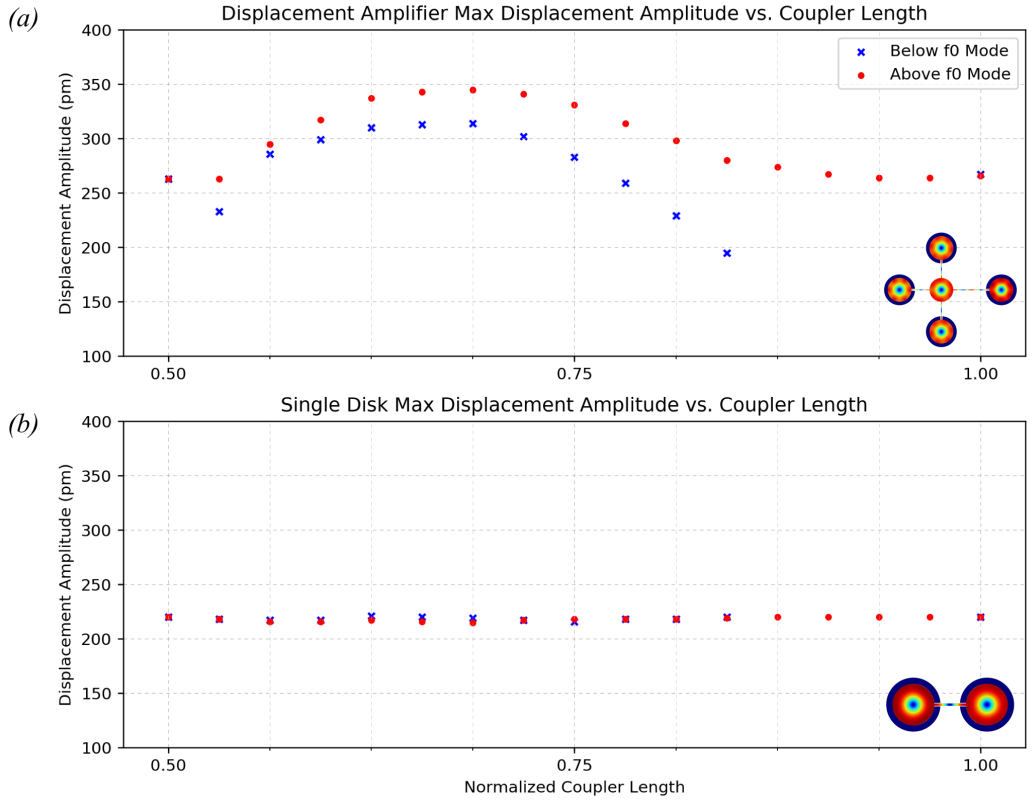

Figure 13: (a) Displacement amplifier and (b) single disk coupled pair max displacement amplitude vs. coupler length.

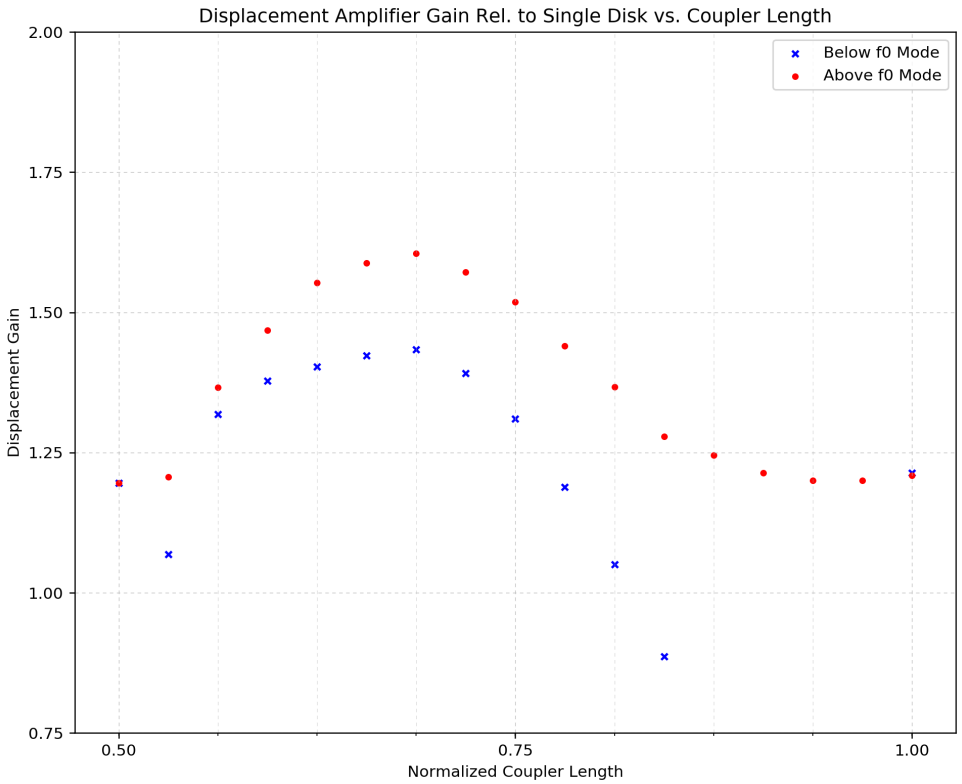

Figure 14: Displacement gain relative to single disk vs. coupler length.

From these curves, a peak displacement is visible at 11/16λ which achieves a displacement 1.6x higher than that of a single input disk. At this peak displacement, as in the eigenfrequency plots, the output disk to input disk displacement is 1.98, very close to the ideal value.

In an attempt to further increase the output displacement amplitude, a central electrode was added to increase the input η by a factor of 4/3. With this addition, the amplitude of this peak increases to a maximum of 422pm, resulting in a gain of 1.95 over the single input disk. This design can easily be modified in the future through the use of smaller gaps to increase the displacement further to magnitudes sufficient for impacting.

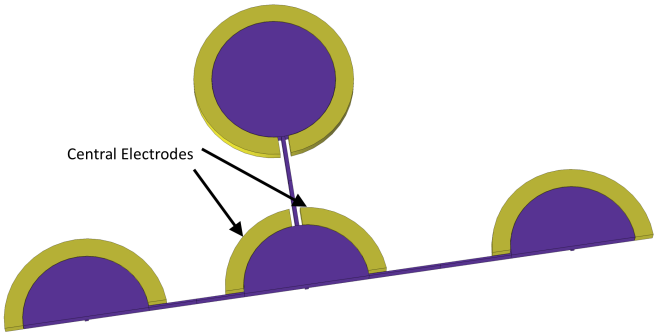

Figure 15: Displacement amplifier with added central electrode to increase driving force and thus maximize output disk displacement.

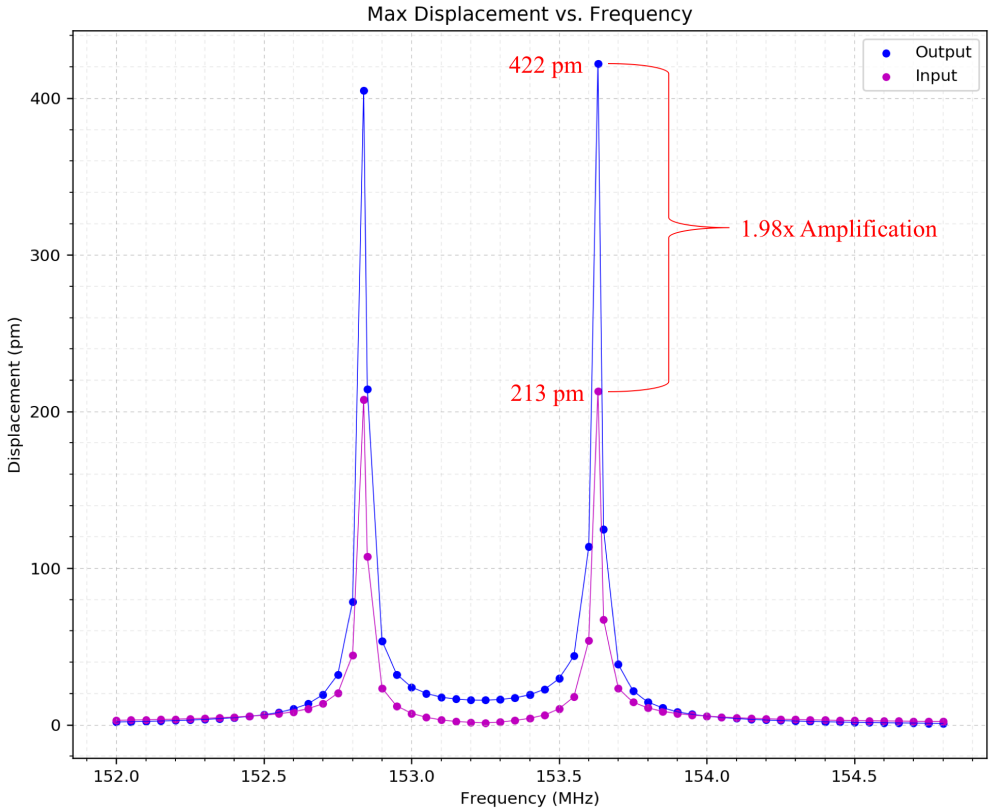

Figure 16: Input and output disk max displacement vs. frequency for output coupler of length 11/16λ, clearly showing a peak displacement gain of approximately 2.

Chapter 5

Conclusion

A thorough analysis using FEA and circuit simulation tools was performed to optimize the gain of a micromechanical resonant displacement amplifier for use in switched power amplifier and converter applications. It was found that a surprisingly accurate match may be obtained between theory and finite element simulation results for such studies, with only a 0.36% difference between theory and simulated measurements.

A maximum displacement amplitude was identified at a coupling length of 11/16λ for the displacement amplifier studied. At this length, a displacement gain of 1.95 is achieved when compared to a single disk. For future resoswitch designs that seek to maximize the gain of the output disk relative to the input, and thus ensure an impact on the output side without an input side impact, this would be the ideal coupler length to use. Deviations from this length result in not only reduced amplitudes, but also in asymmetry between input disk amplitudes that may result in impact on the input side in resoswitch applications.

The high frequency peak of this second order filter was found to produce higher displacements overall than the lower frequency peak, thus being the preferable frequency to target for resoswitch designs. As shown in Figures 13 and 14, this is true for all coupler lengths simulated.

With this knowledge in hand, newer designs may be more readily optimized for higher displacements, which would result in more reliable resoswitch performance. By decreasing the gap size of the design in Figure 15 from 100 nm to 20 nm, with an applied dc bias of 10 V, impact can be achieved with an input voltage of only 120 mV. This design methodology may also be applied towards designs that utilize other types of micromechanical resonators, such as the design of Figure 17, which uses clamped-clamped beams instead of disk resonators. This displacement amplifier topology is a prime target for switched converted and power amplifier applications, and it is hoped that in the future, such designs may be used to produce extremely efficient systems.

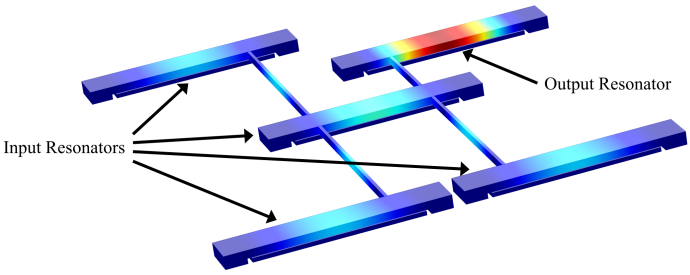

Figure 17: Clamped-clamped beam-based resonant displacement amplifier.

References

[1] P. D. Grant, M.W. Denhoff, and R. R. Mansour, “A Comparison Between RF MEMS Switches and Semiconductor Switches,” in *ICMENS 2004*, pp. 515-521.

[2] Y. Lin, W.-C. Li, Z. Ren, C. T.-C. Nguyen, “The Micromechanical Resonant Switch (“Resoswitch”),” *Tech. Digest*, 2008 Solid-State Sensor, Actuator, and Microsystems Workshop, Hilton Head, South Carolina, pp. 40-43, June 2008.

[3] Y. Lin, W.-C. Li, Z. Ren, and C. T.-C. Nguyen, “A Resonance Dynamical Approach to Faster, More Reliable Micromechanical Switches," in *IEEE Frequency Control Symposium*, Honolulu, Hawaii, USA, 2008, pp. 640-645.

[4] B. Kim, Y. Lin, W.-L. Huang, M. Akgul, W.-C. Li, Z. Ren, and C. T.-C. Nguyen, "Micromechanical Resonant Displacement Gain Stages," in *Proceedings*, 22nd Int. IEEE MEMS Conf., Sorrento, Italy, Jan. 25-29, 2009, pp. 19-22.

[5] Y. Lin, W.-C. Li, I. Gurin, S.-S. Li, Y.-W. Lin, Z. Ren, B. Kim, and C. T.-C. Nguyen, “Digitally-Specified Micromechanical Displacement Amplifiers,” in *Transducers 2009*, pp. 781-784, June 2009.

[6] R. A. Johnson, *Mechanical Filters in Electronics*. New York: Wiley, 1983.

[7] M. Onoe, “Contour Vibrations of Isotropic Circular Plates,” *J. Acoust. Soc. Amer*., vol. 28, pp. 1158–1162, Nov. 1956.

[8] J. R. Clark, W.-T. Hsu, M. A. Abdelmoneum, and C. T.-C. Nguyen, “High-Q UHF Micromechanical Radial-Contour Mode Disk Resonators,”, *J. Microelectromech. Syst*., vol. 14, no. 6, pp. 1298-1310, Dec. 2005.

[9] J. Wang, Z. Ren, and C. T.-C. Nguyen, “1.156-GHz Self-Aligned Vibrating Micromechanical Disk Resonator,”, *IEEE Trans. on Ultrason., Ferroelect., and Freq. Contr*., vol. 51, no. 21, pp. 1607-1628, Dec. 2004.

[10] M. Konno and H. Nakamura, “Equivalent Electrical Network for the Transversely Vibrating Uniform Bar*,” J. Acoust. Soc. Amer*., vol. 38, pp. 614–622, Oct. 1965.

[11] F. D. Bannon III, J.R. Clark, and C. T.-C. Nguyen, "High-Q HF Micromechanical Filters," *IEEE J. Solid- State Circuits*, vol. 35, no. 4, pp. 512-526, April 2000.

[12] A. I. Zverev, *Handbook of Filter Synthesis*. New York: Wiley, 1967.

Appendix

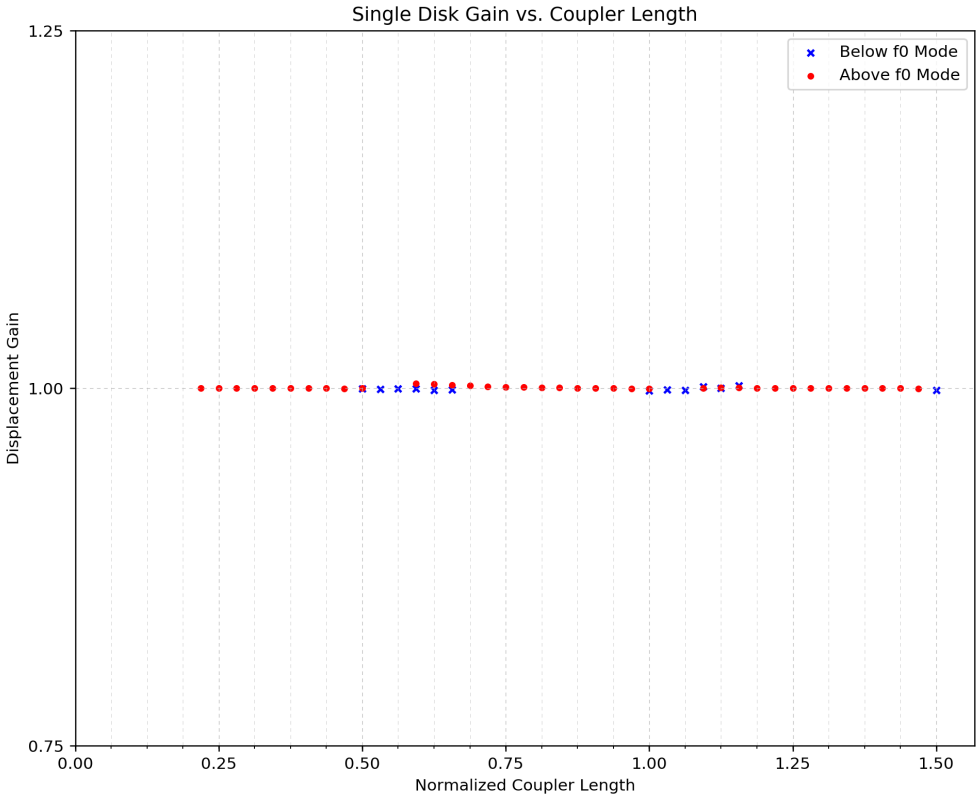

Figure 18: Eigenfrequency study displacement gain plot for single input disk amplifier.

Python Program for Equivalent Circuit Calculations

```
# Disk_Resonator.py
# This program calculates the equivalent circuit parameters for a disk resonator.
# It returns an object with methods for outputting text netlist files to simulate
# impedance and gain using ngspice.
import numpy as np
from numpy import pi, sqrt, sin, cos, tan, sinh, cosh
from scipy import special, integrate, optimize
import matplotlib.pyplot as plt
import subprocess
import os

class disk:
    def __init__(
            self, name, f0_nom, t, d0, Vp, Vi, fi, Q, material, R, Wc, lamda, Lc, N):
        # Material Constants
        e0 = 8.854*10**-12      # Permittivity [F/m]
        if material == 1:
```

```
    E = 150*10**9          # Elastic Modulus [Pa]
    sigma = 0.226          # Poisson's ratio
    rho = 2300             # Density [kg/m^3]
    vel_ac = 8024          # Acoustic Velocity [m/s]
elif material == 2:
    E = 1144*10**9         # Elastic Modulus [Pa]
    sigma = 0.07           # Poisson's ratio
    rho = 3500             # Density [kg/m^3]
    vel_ac = 18076         # Acoustic Velocity [m/s]
elif material == 3:
    E = 415*10**9          # Elastic Modulus [Pa]
    sigma = 0.17           # Poisson's ratio
    rho = 3120             # Density [kg/m^3]
    vel_ac = 11500         # Acoustic Velocity [m/s]
elif material == 4:
    E = 146*10**9          # Elastic Modulus [Pa]
    sigma = 0.2            # Poisson's ratio
    rho = 4280             # Density [kg/m^3]
    vel_ac = 5840          # Acoustic Velocity [m/s]
elif material == 5:
    E = 195*10**9          # Elastic Modulus [Pa]
    sigma = 0.31           # Poisson's ratio
    rho = 8900             # Density [kg/m^3]
    vel_ac = 4678          # Acoustic Velocity [m/s]
elif material == 6:
    E = 70*10**9           # Elastic Modulus [Pa]
    sigma = 0.32           # Poisson's ratio
    rho = 2700             # Density [kg/m^3]
    vel_ac = 6300          # Acoustic Velocity [m/s]

# Calculations
w0_nom = f0_nom*2*pi

h = sqrt(w0_nom**2*rho/(E/(1+sigma) + E*sigma/(1-sigma**2)))
m_re_integral = integrate.quad(lambda r: r*(special.jv(1,h*r))**2,0,R)
m_re = 2*pi*rho*t*m_re_integral[0] / ( (special.jv(1,h*R))**2 )
k_m = w0_nom**2*m_re
c_re = w0_nom*m_re/Q

k_e = (Vp**2+Vi**2/2)*e0*fi*R*t/d0**3

k_re = k_m - k_e

w0 = w0_nom*sqrt(1-k_e/k_m)
f0 = w0/(2*pi)

dcdr = e0*fi*R*t/d0**2
eta12 = Vp*dcdr*(N-1)
eta21 = Vp*dcdr

C01 = (N-1)*e0*t*fi*R/d0
C02 = e0*t*fi*R/d0

Lx1 = N*m_re/(eta12*eta21)
Cx1 = (eta12*eta21)/k_re/N
Rx1 = N*c_re/(eta12*eta21)
```

```
    Lx2 = m_re/(eta12*eta21)
    Cx2 = (eta12*eta21)/k_re
    Rx2 = c_re/(eta12*eta21)

    Z0 = 1/(t*Wc*sqrt(rho*E))
    alpha = w0/sqrt(E/rho)

    ksa = w0*(cos(alpha*Lc) - 1) / (Z0*sin(alpha*Lc))
    ksb = ksa
    ksc = w0/(Z0*sin(alpha*Lc))

    Csa = eta12*eta21/ksa
    Csb = eta12*eta21/ksb
    Csc = eta12*eta21/ksc

    self.f0_nom = f0_nom
    self.f0 = f0
    self.w0_nom = w0
    self.w0 = w0
    self.lamda = lamda
    self.Lc = Lc
    self.t = t
    self.d0 = d0
    self.N = N
    self.Vp = Vp
    self.Vi = Vi
    self.fi = fi
    self.Q = Q
    self.E = E
    self.vel_ac = vel_ac
    self.rho = rho
    self.R = R
    self.m_re = m_re
    self.k_m = k_m
    self.k_e = k_e
    self.k_re = k_re
    self.c_re = c_re
    self.eta12 = eta12
    self.eta21 = eta21
    self.C01 = C01
    self.C02 = C02
    self.Lx1 = Lx1
    self.Cx1 = Cx1
    self.Rx1 = Rx1
    self.Lx2 = Lx2
    self.Cx2 = Cx2
    self.Rx2 = Rx2
    self.Csa = Csa
    self.Csb = Csb
    self.Csc = Csc
    self.name = name

def printout(self):
    print("\n----------------", self.name, "Resonator Results ----------------")
    print("f0     =", '%9.2f' % (self.f0*10**-6), "MHz")
```

```
    print("Radius =", '%9.3E' % (self.R*10**6), "um")
    print("t      =", '%9.3E' % (self.t*10**6), "um")
    print("k_m    =", '%9.3E' % self.k_m, "N/m", "    k_e   =", '%.3E' % self.k_e,
        "N/m")
    print("k_re   =", '%9.3E' % self.k_re, "N/m")
    print("m_re   =", '%9.3E' % self.m_re, "kg")
    print("c_re   =", '%9.3E' % self.c_re, "kg/s")
    print("eta12    =", '%9.3E' % self.eta12)
    print("eta21    =", '%9.3E' % self.eta21)
    print("Rx1     =", '%9.3E' % self.Rx1, "ohms")
    print("Lx1     =", '%9.3E' % self.Lx1, "H")
    print("Cx1     =", '%9.3E' % (self.Cx1*10**15), "fF")
    print("Rx2     =", '%9.3E' % self.Rx2, "ohms")
    print("Lx2     =", '%9.3E' % self.Lx2, "H")
    print("Cx2     =", '%9.3E' % (self.Cx2*10**15), "fF")

    print("Csa     =", '%9.3E' % (self.Csa*10**15), "fF")
    print("Csb     =", '%9.3E' % (self.Csb*10**15), "fF")
    print("Csc     =", '%9.3E' % (self.Csc*10**15), "fF")

    print("C01     =", '%9.3E' % (self.C01*10**15), "fF")
    print("C02     =", '%9.3E' % (self.C02*10**15), "fF\n")

def makenetlist_gain(self, RQ1, RQ2):
    if not(os.path.isdir(os.getcwd() + "/netlists")):
        subprocess.call(['mkdir', 'netlists'])
    netlist = open('./netlists/' + self.name + '.cir', 'w')
    netlist.write(self.name)

    netlist.write('\nVin 0 n002 dc 0 ac 1')
    netlist.write('\nRq1 0 n002 ' + str(RQ1))

    netlist.write('\nRx1 n002 n003 ' + str(self.Rx1))
    netlist.write('\nCx1 n003 n004 ' + str(self.Cx1))
    netlist.write('\nLx1 n004 n005 ' + str(self.Lx1))

        # Coupling capacitors
    netlist.write('\nCsa n005 n006 ' + str(self.Csa))
    netlist.write('\nCsb n006 n007 ' + str(self.Csb))
    netlist.write('\nCsc n006 0 ' + str(self.Csc))

        # Shunt resistors for coupling caps
    netlist.write('\nRshunt_a n005 n006 100T')
    netlist.write('\nRshunt_b n006 n007 100T')
    netlist.write('\nRshunt_c n006 0 100T')

    netlist.write('\nRx2 n007 n008 ' + str(self.Rx2))
    netlist.write('\nCx2 n008 n009 ' + str(self.Cx2))
    netlist.write('\nLx2 n009 vout ' + str(self.Lx2))

    netlist.write('\nC01 n002 0 ' + str((self.C01)))
    netlist.write('\nC02 vout 0 ' + str((self.C02)))

    netlist.write('\nRq2 vout 0 ' + str(RQ2))

    netlist.write('\n.control')
```

```
    netlist.write('\nac dec 3000 1 10000G')
    netlist.write('\nset filetype=ascii')
    if not(os.path.isdir(os.getcwd() + "/data")):
        subprocess.call(['mkdir', 'data'])
    netlist.write('\nwrdata ./data/' +self.name + '_freqresp_vout' + ' mag(vout)')
    netlist.write('\nac lin 5000 ' + str(self.f0*0.98) + ' '
          + str(self.f0*1.02))
    netlist.write('\nwrdata ./data/' +self.name + '_peak_vout' + ' mag(vout)')
    netlist.write('\nquit')
    netlist.write('\n.endc')
    netlist.write('\n.end')
    netlist.close()

def makenetlist_inputimpedance(self, RQ1, RQ2, Rs):
    if not(os.path.isdir(os.getcwd() + "/netlists")):
        subprocess.call(['mkdir', 'netlists'])
    netlist = open('./netlists/' + self.name + '_input_impedance.cir', 'w')
    netlist.write(self.name)

    netlist.write('\nIin 0 n001 dc 0 ac 1')
    netlist.write('\nVs n001 n010 dc 0')
    netlist.write('\nRs n010 n002 ' + str(Rs))

    # Note that this RQ1 is used as a shunt resistor
    netlist.write('\nRq1 n002 0 ' + str(RQ1))

    netlist.write('\nRx1 n002 n003 ' + str(self.Rx1))
    netlist.write('\nCx1 n003 n004 ' + str(self.Cx1))
    netlist.write('\nLx1 n004 n005 ' + str(self.Lx1))

        # Coupling capacitors
    netlist.write('\nCsa n005 n006 ' + str(self.Csa))
    netlist.write('\nCsb n006 n007 ' + str(self.Csb))
    netlist.write('\nCsc n006 0 ' + str(self.Csc))

        # Shunt resistors for coupling caps to set bias point
    netlist.write('\nRshunt_a n005 n006 100T')
    netlist.write('\nRshunt_b n006 n007 100T')
    netlist.write('\nRshunt_c n006 0 100T')

    netlist.write('\nRx2 n007 n008 ' + str(self.Rx2))
    netlist.write('\nCx2 n008 n009 ' + str(self.Cx2))
    netlist.write('\nLx2 n009 vout ' + str(self.Lx2))

    netlist.write('\nC01 n002 0 ' + str((self.C01)))
    netlist.write('\nC02 vout 0 ' + str((self.C02)))

    netlist.write('\nRq2 vout 0 ' + str(RQ2))

    netlist.write('\n.control')
    netlist.write('\nset filetype=ascii')
    if not(os.path.isdir(os.getcwd() + "/data")):
        subprocess.call(['mkdir', 'data'])
    netlist.write('\nac lin 20000 149MEG 162MEG')
    netlist.write('\nwrdata ./data/' +self.name + '_input_impedance' + ' mag(v(n002)/i(Vs))')
    netlist.write('\nquit')
```

```
    netlist.write('\n.endc')
    netlist.write('\n.end')
    netlist.close()

def makenetlist_outputimpedance(self, RQ1, RQ2, Rs):
    if not(os.path.isdir(os.getcwd() + "/netlists")):
        subprocess.call(['mkdir', 'netlists'])
    netlist = open('./netlists/' + self.name + '_output_impedance.cir', 'w')
    netlist.write(self.name)

    netlist.write('\nIin 0 n001 dc 0 ac 1')
    netlist.write('\nVs n001 n010 dc 0')
    netlist.write('\nRs n010 vout ' + str(Rs))

    netlist.write('\nRq1 n002 0 ' + str(RQ1))

    netlist.write('\nRx1 n002 n003 ' + str(self.Rx1))
    netlist.write('\nCx1 n003 n004 ' + str(self.Cx1))
    netlist.write('\nLx1 n004 n005 ' + str(self.Lx1))

        # Coupling capacitors
    netlist.write('\nCsa n005 n006 ' + str(self.Csa))
    netlist.write('\nCsb n006 n007 ' + str(self.Csb))
    netlist.write('\nCsc n006 0 ' + str(self.Csc))

        # Shunt resistors for coupling caps to set bias point
    netlist.write('\nRshunt_a n005 n006 100T')
    netlist.write('\nRshunt_b n006 n007 100T')
    netlist.write('\nRshunt_c n006 0 100T')

    netlist.write('\nRx2 n007 n008 ' + str(self.Rx2))
    netlist.write('\nCx2 n008 n009 ' + str(self.Cx2))
    netlist.write('\nLx2 n009 vout ' + str(self.Lx2))

    netlist.write('\nC01 n002 0 ' + str((self.C01)))
    netlist.write('\nC02 vout 0 ' + str((self.C02)))

    # Note that this RQ2 is used as a shunt resistor
    netlist.write('\nRq2 vout 0 ' + str(RQ2))

    netlist.write('\n.control')
    netlist.write('\nset filetype=ascii')
    if not(os.path.isdir(os.getcwd() + "/data")):
        subprocess.call(['mkdir', 'data'])
    netlist.write('\nac lin 20000 149MEG 162MEG')
    netlist.write('\nwrdata ./data/' +self.name + '_output_impedance' + ' mag(v(vout)/i(Vs))')
    netlist.write('\nquit')
    netlist.write('\n.endc')
    netlist.write('\n.end')
    netlist.close()
```